2014 IEEE Congress on Evolutionary Computation (CEC)
July 6-11, 2014, Beijing, China

The Coupled EigenAnt algorithm for shortest path problems

Eugenius Kaszkurewicz, Amit Bhaya, Jayadeva, João Marcos Meirelles da Silva

Abstract— **This paper introduces an ACO model and associated algorithm, called Coupled EigenAnt, for the problem of finding the shortest of N paths between a source and a destination node. It is based on the recently introduced EigenAnt algorithm, the novelty being that it allows probabilistic path choice on both the forward and return journeys, as well as the fact that it introduces decay of pheromone deposition following a geometric progression. Equilibrium points of the model are calculated and the local stability of the two path synchronous version analyzed. Simulations illustrate the main features of the algorithm.**

I. Introduction

IT is only a mild exaggeration to say that ant colony optimization (ACO) algorithms are almost as varied as species of biological ants. However, some paradigms have already been established. For practical computational reasons, Dorigo and Stützle [1, p.11] propose simple-ACO or S-ACO ants featuring probabilistic path selection on the forward journey, with path choice probabilities given by relative pheromone concentrations, and deposition of pheromone only on the return journey, thus assuming that, once a path has been chosen for the forward voyage (also referred to as source to destination, or nest to food), it is necessarily chosen for the return journey. This is a common assumption for many ACO algorithms, although Dorigo and Stützle [1, p.6, ff.] write: "if we consider a model in which ants deposit pheromone only during the forward or only during the backward trip, then the result is that the ant colony is unable to choose the shortest branch. The observation of real ant colonies has confirmed that ants that deposit pheromone only when returning to the nest are unable to find the shortest path between their nest and the food source [2]." Motivated by this observation, in this paper, we propose a simple model that allows probabilistic path selection, as well as pheromone deposition on both the forward and return journeys.

The amount of artificial pheromone deposited on a path depends on its length: the shorter the path, the greater the amount of added pheromone. This dependence is usually achieved by making the deposition parameter of each path inversely proportional to its length. In order to achieve plasticity (the ability to switch to a shorter path when it becomes available), the deposited pheromone is subjected either to evaporation, which corresponds to pheromone removal at a fixed rate on all paths, or, in more recent work, removal that is only caused by ant traffic on a given path. It should be emphasized that although all the features, mentioned in this and the preceding paragraph, bear some resemblance to the behavior of real ants, their main justification is that they enable artificial ants to carry out some useful computation, typically finding the solution of a shortest path problem.

In recent work, Jayadeva et al. [3] proposed the EigenAnt dynamics for deposition and removal of pheromone by a single ant that is required to find the shortest of N paths between a source and a destination. They maintained the usual assumption of deposition only on the return journey, but introduced a dependency on normalized pheromone concentration in the deposition term. Deterministic (averaged) EigenAnt dynamics was shown to have only one stable equilibrium point, and the EigenAnt algorithm based on this discrete-time dynamics was simulated, indicating that, even under the usual probabilistic asynchronous implementation, convergence occurs to the equilibrium that corresponds to the shortest path. A model similar to EigenAnt was also studied in [4]. Later, Bliman et al. [5] established global asymptotic stability of this equilibrium for continuous-time deterministic EigenAnt dynamics.

The EigenAnt algorithm was aptly referred to as a bare bones algorithm in [6], which successfully incorporated it into the larger setting of ACO metaheuristics for solving multiple node shortest path problems such as the sequential ordering problem. The reason for the bare bones terminology is that EigenAnt has only two parameters and, crucially, because of the global convergence property for all parameter choices, its performance is not critically dependent on these parameters.

This paper proposes to examine some of the basic assumptions in the ACO literature from a bare bones EigenAnt-like perspective. Specifically, we consider once again the simple paradigmatic one ant, two node shortest path problem. The discrete-time dynamics that we propose constitutes a new variant of the EigenAnt dynamics and is referred to as the coupled EigenAnt model, since it couples EigenAnt-like dynamics at the source and destination nodes by permitting probabilistic path selection at both source and destination, in accordance with the biological motivation mentioned above. We assume that paths are chosen probabilistically, using roulette wheel selection (RWS) based on path pheromone concentrations. Moreover, RWS can occur only at the source (in this case, the return journey occurs on the same path as the forward journey, as in the EigenAnt model), or at both the source and the destination, which constitutes one of the novelties in the Coupled EigenAnt model being proposed in

EK and AB are with the Department of Electrical Engineering (email: {eugenius, amit}@nacad.ufrj.br). Jayadeva is with the Electrical Engineering Department, Indian Institute of Technology, Delhi, India (e-mail: jayadeva@ee.iitd.ac.in). JMMS is with the Department of Telecommunications Engineering of the Federal Fluminense University (e-mail: jmarcos@telecom.uff.br).

This work was supported by BPP/CNPq grants to EK, AB and a joint Indo-Brazil DST/CNPq grant to AB and J.

978-1-4799-1488-3/14/$31.00 ©2014 IEEE

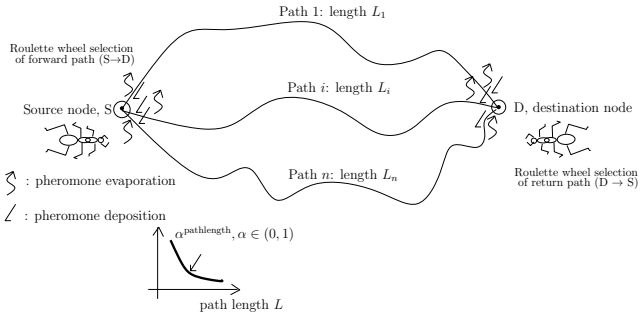

Fig. 1: Shortest path problem set up.

this paper.

Although the equilibrium point structure of EigenAnt is maintained, the unique equilibrium that corresponds to the shortest path is no longer globally stable, so that, in the Coupled EigenAnt model, there exist deposition and removal parameters for which convergence to a local minimum may not occur. Also, analogously to the results in [3], the coupled EigenAnt model is compared to a coupled S-ACO type model and shown to have better performance. Specifically, our simulations indicate that the following performance hierarchy exists Coupled EigenAnt (RWS at source and destination) > Coupled EigenAnt (RWS at source only) > S-ACO (RWS at source and destination) > S-ACO (RWS at source only).

Section II sets up the basic problem and defines notation. Section III introduces the basic model as well as the associated algorithm. Section IV calculates the equilibria of the proposed dynamics, and then discusses local stability analysis for the two-node, two-path problem. Section V presents simulation results. Finally, section VI makes some concluding remarks.

II. Problem setup and notation

A. Notation

- pheromone concentration is abbreviated pc.
- Source: S.
- Destination: D.
- pc at S on path i: σ_i.
- pc at D on path i: τ_i.
- pc vector at S is denoted $\boldsymbol{\sigma}$.
- pc vector at D is denoted $\boldsymbol{\tau}$.
- trip counter: m
- length of path i: L_i.
- number of paths: N.
- Pheromone deposition parameter: α.
- Pheromone removal parameter: ρ.
- Integers k_i proportional to path lengths L_i.
- Roulette wheel selection: RWS
- $\mathbb{1} \in \mathbb{R}^N$: vector of ones.

III. The coupled EigenAnt model

In their seminal paper on chemical communication, Bossert and Wilson [7] wrote "The essential goals of a short-lived recruitment trail have been intuited as follows. The amount of material emitted at any instant of time must not be very great, because in a typical circumstance the material must be emitted over a relatively long distance out of a reservoir of finite capacity." Inspired by this as well as the ACO literature, we propose a simple model of an artificial ant which deposits a quantity of pheromone that decreases in geometric progression as the ant proceeds along the trail. In addition, the usual ingredients of removal and probabilistic path selection are present.

Suppose that a pheromone deposition rate is given in the following manner. Starting from a full reservoir of pheromone (say 1 unit), as the ant proceeds along the trail, in the first step after starting out from the nest, it deposits $1-\alpha$ units and, in the nth subsequent step, a quantity of pheromone that has decreased in geometric progression, i.e., $(1-\alpha)^n$. Suppose that k_i is the exponent associated to the ith path in the sense that, after one trip on this path, starting from a full reservoir (1 unit) of pheromone at one end, the ant deposits $(1-\alpha)^{k_i}$ units of pheromone on reaching the other end. Let the exponent vector be denoted $\mathbf{k}$, i.e., $\mathbf{k} = [k_1\ k_2\ \cdots k_N]$.

In order to define pheromone deposition and removal, it is necessary to make some assumption on the exponents k_i and, for simplicity, we make the assumption that $k_i = L_i$, which implies that pheromone deposition decreases in geometric progression in accordance with the path length, so that longer paths have less pheromone deposited at their end points.

The program (algorithm/environment) has knowledge of the vector $\mathbf{k}$, but the ant itself does not. We postulate, in common with the literature on ACO, that an ant has the capacity to distinguish between relative pheromone concentrations. More precisely, we assume that if the pheromone concentration vector $\boldsymbol{\tau} = [\tau_1 \quad \cdots \quad \tau_n]$ is associated to the n paths, then an ant chooses path i with probability $\tau_i / \sum_j \tau_j$. Suppose that path i is chosen for the forward (S to D) journey and path j for the return (D to S) journey and that the superscript $+$ denotes the update of a pheromone concentration.

The model of pheromone deposition and removal dynamics that we propose in this paper is as follows. The Coupled EigenAnt model

$$\tau_i^+ = (1-\rho)^{k_i}\tau_i + (1-\alpha)^{k_i}\frac{\sigma_i}{\sum_\ell \sigma_\ell} \tag{1}$$

$$\sigma_j^+ = (1-\rho)^{k_j}\sigma_j + (1-\alpha)^{k_j}\frac{\tau_j}{\sum_\ell \tau_\ell}, \tag{2}$$

The procedure that we propose, for a single ant carrying out N trips (the journey S → D, D → S counts as 1 trip) is then described, for the Coupled EigenAnt model, in the two roulette case, as follows:

1) The ant emerging from node S chooses path i with probability $\sigma_i / \sum_j \sigma_j$ (RWS at S). Having chosen path i, it deposits, at the node D, when it gets there, the quantity $(1-\alpha)^{k_i}$ times the normalized pheromone concentration at S. Pheromone removal $(1-\rho)^{k_i}$ occurs at D only on the ith path. Summing the concentration due to deposition and that remaining after removal, the

overall concentration at D, on path i, is updated to τ_i^+, which is (1).

2) On emerging from D to return to S, it chooses a path probabilistically (say the jth) as in step 1 (RWS at D), using the updated pheromone concentrations. Having chosen path j, it deposits, at the node S when it gets there, the quantity $(1-\alpha)^{k_j}$ times the normalized pheromone concentration at D. The corresponding removal $(1-\rho)^{k_j}$ occurs at S on the jth path only. The pheromone concentration vector at S, on path j, is updated by the summation analogous to the one described in the previous item, i.e., (2).
3) Steps 1 and 2 are repeated M times.
4) The program keeps track of how many times each path is chosen, as well as ranking the paths in order of pheromone concentration.
5) The program outputs a path counter vector that indicates how many times each path is chosen, as well as the normalized pheromone concentrations at source and destination (which are equal at equilibrium).

The pseudocode corresponding to this procedure is shown as Algorithm 1.

To exemplify the use of this procedure to solve a shortest path problem, in which the program plays the part of the environment (black box), suppose that we grid α and ρ and to each pair $1-\alpha, \rho$, we associate the smallest value of number of steps found in M executions of the program, called k_{low}. The surface plot of $1-\alpha, \rho$ versus k_{low} has a minimum called $k_{\min}$, which is declared to be the number of steps corresponding to the shortest path (which we can translate into an estimate of the length $L_{\min}$, in accordance with the relationship assumed to hold between k_i and L_i).

In the algorithm below, comments appear to the right of the symbol ▷.

Algorithm 1 Coupled EigenAnt algorithm with S & D roulettes

$m := 0$ ▷ Trip counter initialized
Path trip counter initialized to zero for all paths.
$\boldsymbol{\sigma} = \boldsymbol{\tau} = (1/N)\mathbb{1}$. ▷ Initialize pc at S & D
while $m \neq$ maximum number (M) of trips **do**
  Choose path index i by RWS based on pc at S.
  Increment path i trip count by 1.
  $\tau_i \leftarrow (1-\rho)^{k_i}\tau_i$ ▷ pc update at D
  $\tau_i \leftarrow \tau_i + (1-\alpha)^{k_i}\frac{\sigma_i}{\sum_\ell \sigma_\ell}$ ▷ pc update on path i
  Choose path index j by RWS based on pc at D.
  Increment path j trip count by 1.
  $\sigma_j \leftarrow (1-\rho)^{k_j}\sigma_j$ ▷ pc update at S
  $\sigma_j \leftarrow \sigma_j + (1-\alpha)^{k_j}\frac{\tau_j}{\sum_\ell \tau_\ell}$. ▷ pc update on path j
  $m \leftarrow m+1$
end while
Return $\boldsymbol{\sigma}$ and path trip counter vector.

Connections with existing models: Algorithm 1, with all exponents $k_i = 1$, $1-\alpha_i = \gamma/L_i$ and only the S roulette (so that the return path j is equal to the forward path i) is equivalent to the EigenAnt algorithm proposed in [3]. Algorithm 2, with all exponents $k_i = 1$, $(1-\alpha_i = Q/L_i$ and only the S-roulette is equivalent to the S-ACO algorithm described in [1], [8].

Algorithm 2 S-ACO algorithm with S & D roulettes

$m := 0$ ▷ Trip counter initialized
Path trip counter initialized to zero for all paths.
$\boldsymbol{\sigma} = \boldsymbol{\tau} = (1/N)\mathbb{1}$. ▷ Initialize pc at S & D
while $m \neq$ maximum number (M) of trips **do**
  Choose path index i by RWS based on pc at S.
  Increment path i trip count by 1.
  $\tau_i \leftarrow (1-\rho)^{k_i}\tau_i$ ▷ pc update at D
  $\tau_i \leftarrow \tau_i + (1-\alpha)^{k_i}$ ▷ pc update on path i
  Choose path index j by RWS based on pc at D.
  Increment path j trip count by 1.
  $\sigma_j \leftarrow (1-\rho)^{k_j}\sigma_j$ ▷ pc update at S
  $\sigma_j \leftarrow \sigma_j + (1-\alpha)^{k_j}$. ▷ pc update on path j
  $m \leftarrow m+1$
end while
Return $\boldsymbol{\sigma}$ and path trip counter vector.

IV. Analysis of equilibria and their stability

This section is devoted to determining the equilibrium points for the coupled EigenAnt model described by (1), (2) and Algorithm 1, assuming that pheromone concentrations on all paths are updated simultaneously (synchronously) for the forward and return journeys. Let us denote the constants

$$r_i = (1-\rho)^{k_i} \tag{3}$$
$$a_i = (1-\alpha)^{k_i} \tag{4}$$

and define the diagonal matrices $\mathbf{A} = \text{diag}(a_1, \ldots, a_N)$ and $\mathbf{R} = \text{diag}(r_1, \ldots, r_N)$. Then, writing $\sum_i x_i$ as $\mathbb{1}^\intercal \mathbf{x}$ for typographical convenience when necessary, we can write the synchronous fixed point equation corresponding to (1), (2) as follows:

$$\boldsymbol{\tau} = \mathbf{R}\boldsymbol{\tau} + (1/\mathbb{1}^\intercal\boldsymbol{\sigma})\,\mathbf{A}\boldsymbol{\sigma} \tag{5}$$
$$\boldsymbol{\sigma} = \mathbf{R}\boldsymbol{\sigma} + (1/\mathbb{1}^\intercal\boldsymbol{\tau})\,\mathbf{A}\boldsymbol{\tau} \tag{6}$$

Solving (5) for $\boldsymbol{\tau}$ in terms of $\boldsymbol{\sigma}$ yields:

$$\boldsymbol{\tau} = (1/\mathbb{1}^\intercal\boldsymbol{\sigma})\,(\mathbf{I}-\mathbf{R})^{-1}\mathbf{A}\boldsymbol{\sigma} \tag{7}$$

Using the fact that diagonal matrices commute, the equation to be satisfied by any equilibrium point $\boldsymbol{\sigma}$ is:

$$\left(\mathbf{I} - \frac{(\mathbf{I}-\mathbf{R})^{-2}\mathbf{A}^2}{\sum_i \sigma_i \sum_i \tau_i}\right)\boldsymbol{\sigma} = \mathbf{0} \tag{8}$$

Suppose that the ith fixed point $\boldsymbol{\sigma}_i^*$ is given by $\mu_i \mathbf{e}_i$, where μ_i is an arbitrary scalar to be determined and $\mathbf{e}_i$ is the ith canonical vector in $\mathbb{R}^N$. Plugging this guess, inspired by [3], into (8), straightforward calculation shows that (8) is indeed satisfied if:

$$\mu_i = \frac{a_i}{1-r_i} \tag{9}$$

and, furthermore, that the equilibria of the synchronous version of the model are given by $\boldsymbol{\sigma}_i^* = \boldsymbol{\tau}_i^* = \mu_i \mathbf{e}_i$. The natural interpretation of this is that the equilibrium pheromone concentrations for this model are the same at source and destination and, since they are multiples of the canonical vectors, occur by singling out one of the N paths on which there is a nonzero concentration, with all other paths having zero concentrations. The stability analysis that follows will indicate how to calculate ranges of the parameters for which local stability of the desired equilibrium, for which all the pheromone is concentrated on the shortest path.

A. Local stability analysis for the two path problem

For the two path problem, we can write the synchronous version of model (1), (2) explicitly as the following system of four coupled discrete-time systems:

$$\begin{aligned}
\sigma_1(k+1) &= r_1\sigma_1(k) + a_1(\tau_1(k)/(\tau_1(k)+\tau_2(k))) \\
\sigma_2(k+1) &= r_2\sigma_2(k) + a_2(\tau_2(k)/(\tau_1(k)+\tau_2(k))) \\
\tau_1(k+1) &= r_1\tau_1(k) + a_1(\sigma_1(k)/(\sigma_1(k)+\sigma_2(k))) \\
\tau_2(k+1) &= r_2\tau_2(k) + a_2(\sigma_2(k)/(\sigma_1(k)+\sigma_2(k)))
\end{aligned}$$

It is easy to check that the two equilibria are indeed given by $\mu_i \mathbf{e}_i$, where μ_i is given by (9). In order to check local stability, we compute the Jacobian matrix $J(\boldsymbol{\sigma}, \boldsymbol{\tau})$ which is:

$$J = \begin{bmatrix}
r_1 & 0 & \frac{a_1\tau_2}{(\tau_1+\tau_2)^2} & -\frac{a_1\tau_1}{(\tau_1+\tau_2)^2} \\
0 & r_2 & -\frac{a_2\tau_2}{(\tau_1+\tau_2)^2} & \frac{a_2\tau_1}{(\tau_1+\tau_2)^2} \\
\frac{a_1\sigma_2}{(\sigma_1+\sigma_2)^2} & -\frac{a_1\sigma_1}{(\sigma_1+\sigma_2)^2} & r_1 & 0 \\
-\frac{a_2\sigma_2}{(\sigma_1+\sigma_2)^2} & \frac{a_2\sigma_1}{(\sigma_1+\sigma_2)^2} & 0 & r_2
\end{bmatrix}$$

If all the magnitudes of the eigenvalues of $J_i := J(\boldsymbol{\sigma}_i^*, \boldsymbol{\tau}_i^*), i = 1, 2$ are less than unity, this implies the local stability of the equilibrium $\boldsymbol{\sigma}_i^* = \boldsymbol{\tau}_i^*, i = 1, 2$.

V. Numerical simulations

In this section, we show the behavior of the model implemented in its asynchronous, probabilistic version, as shown in Algorithm 1. For illustrative purposes, we consider a ten path problem with the path length vector $L = [7, 4, 8, 9, 6, 2, 3, 5, 10, 11]$, we choose $\alpha \in [0.01, 1]$, $\rho \in [0.01, 1]$. The simulations are carried out for 100 ant trips. In order to calculate the probability of successfully finding the shortest path, we use the following procedure. The path counter vector used in both Algorithms 1 and 2, counts the number of times the shortest path is the one that is traversed the most often, over a set of 100 trials, and this number is reported as the success probability.

Comments on the simulations:

From the simulations of success probabilities, the following indications are clear:

1) For both the Coupled EigenAnt and S-ACO algorithms, it is always better to use roulettes at both S and D, rather than only at S. To see this, compare Figure 3 with Figure 7 and Figure 5 with Figure 9, as well as Figure 2 with Figure 6; and Figure 4 with Figure 8.
2) The Coupled EigenAnt algorithms have a better performance than that of the S-ACO algorithms, following the hierarchy Coupled EigenAnt (RWS at source and destination) > Coupled EigenAnt (RWS at source only) > S-ACO (RWS at source and destination) > S-ACO (RWS at source only). To see this, compare Figure 7 with Figures 3, Figure 9, Figure 5 in the order specified.
3) As the simulation horizon (= number of trips) increases, performance of all the algorithms improves, with the Coupled EigenAnt improving its lead over the S-ACO algorithms. A sample of this can be seen by comparing Figures 11 with 13 as well as Figure 10 with 12.

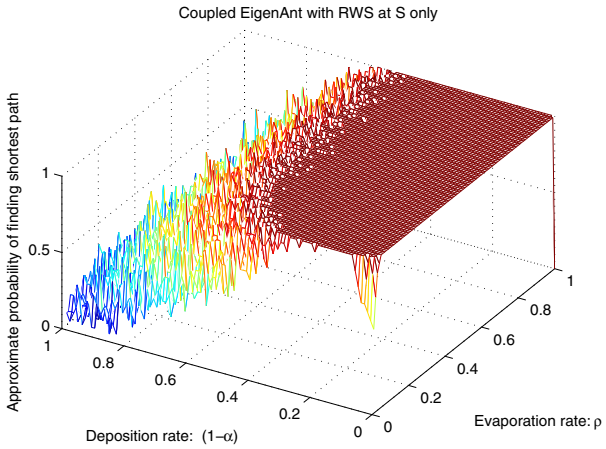

Fig. 2: Success probability as a function of removal and deposition rates for the Coupled EigenAnt algorithm, with flat initial conditions (= no initial bias), RWS at S only, and approximate probabilities based on 100 runs, for the 10 path problem (Elevation view). Simulation horizon of 100 trips.

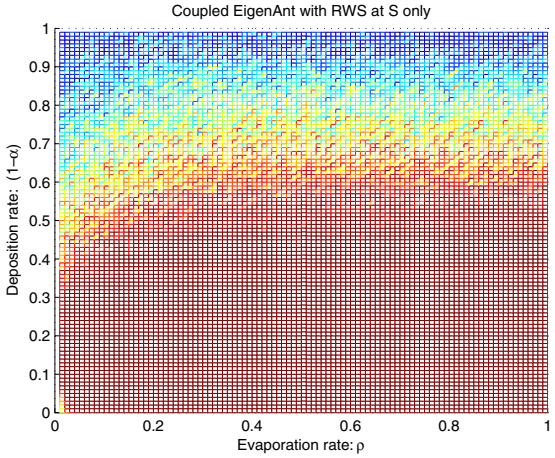

Fig. 3: Success probability as a function of removal and deposition rates for the Coupled EigenAnt algorithm, with flat initial conditions (= no initial bias), RWS at S only, and approximate probabilities based on 100 runs, for the 10 path problem (Plan view). Simulation horizon of 100 trips.

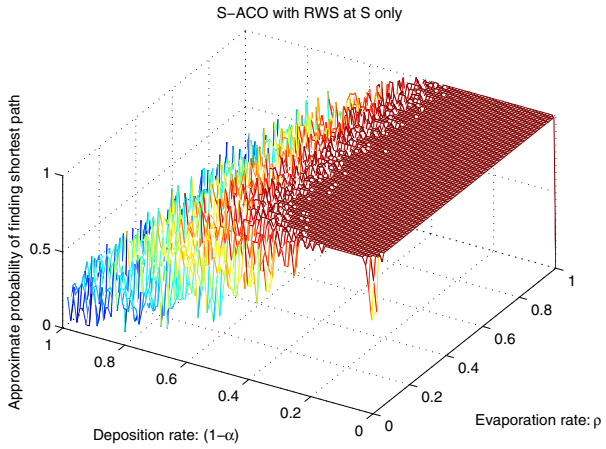

Fig. 4: Success probability as a function of removal and deposition rates for the S-ACO algorithm, with flat initial conditions (= no initial bias), RWS at S only, and approximate probabilities based on 100 runs1, for the 10 path problem (Elevation view). Simulation horizon of 100 trips.

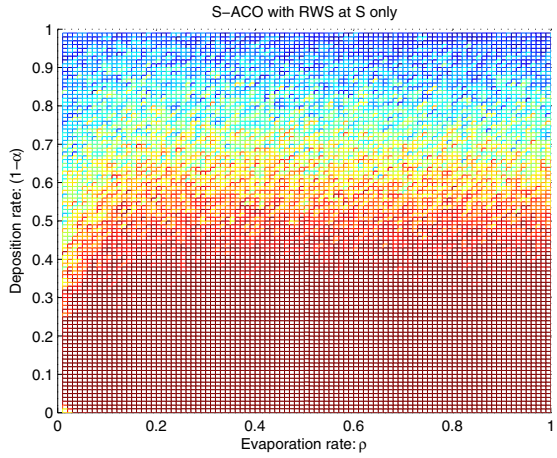

Fig. 5: Success probability as a function of removal and deposition rates for the S-ACO algorithm, with flat initial conditions (= no initial bias), RWS at S only, and approximate probabilities based on 100 runs, for the 10 path problem (Plan view). Simulation horizon of 100 trips.

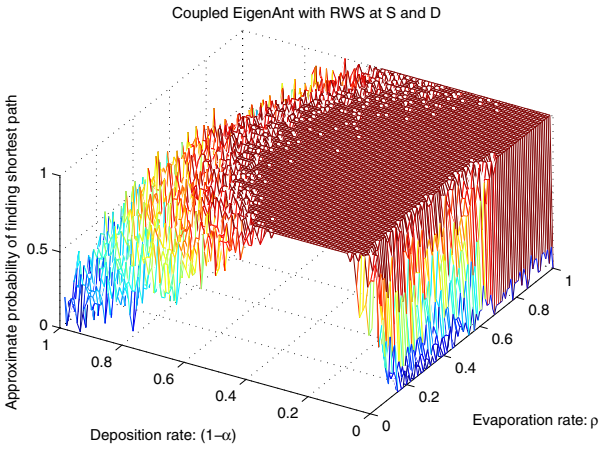

Fig. 6: Success probability as a function of removal and deposition rates for the Coupled EigenAnt algorithm, with flat initial conditions (= no initial bias), RWS at S and D, and approximate probabilities based on 100 runs, for the 10 path problem (Elevation view). Simulation horizon of 100 trips.

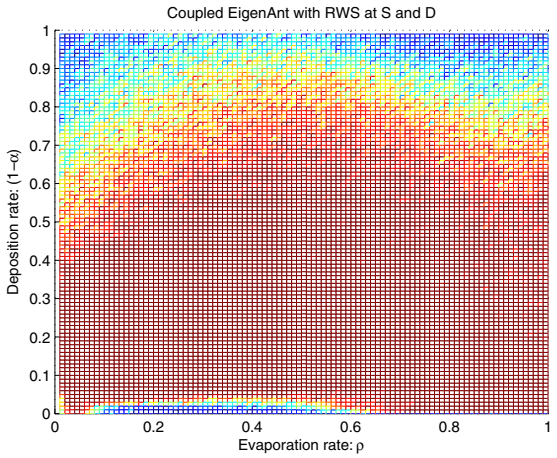

Fig. 7: Success probability as a function of removal and deposition rates for the Coupled EigenAnt algorithm, with flat initial conditions (= no initial bias), RWS at S and D, and approximate probabilities based on 100 runs, for the 10 path problem (Plan view). Simulation horizon of 100 trips.

VI. Concluding Remarks

This paper introduced a new ACO model called the Coupled EigenAnt model, based on the recently introduced EigenAnt model, but allowing probabilistic path choice on both the forward and return journeys, in an attempt to capture similar behavior of real ants. This was shown, by simulation results, to result in better performance than a single probabilistic path choice only on the forward journey. Furthermore, as with the EigenAnt model [3], the Coupled EigenAnt model also exhibits better performance than S-ACO versions which permit one or two probabilistic path choices (i.e., at source and/or destination). The Coupled EigenAnt model proposed in this paper has potential for "real" implementations in which lengths are not known, but there is a signal available indicating that an end node (food or nest) has been reached (the ant must only bookkeep the amount of pheromone it has left in its "bladder" to mark path endpoints. Adjustment of deposition and removal rates, which enter calculations in the algorithm after exponentiation, is important because the resulting values should not become too small (numerically indistinguishable from zero). The model opens up possibilities for many variations that follow the same basic design and some of these will be followed up in future work.

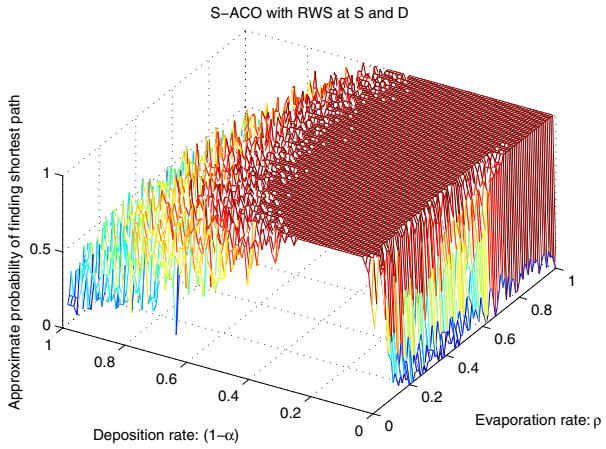

Fig. 8: Success probability as a function of removal and deposition rates for the S-ACO algorithm, with flat initial conditions (= no initial bias), RWS at S and D, and approximate probabilities based on 100 runs, for the 10 path problem (Elevation view). Simulation horizon of 100 trips.

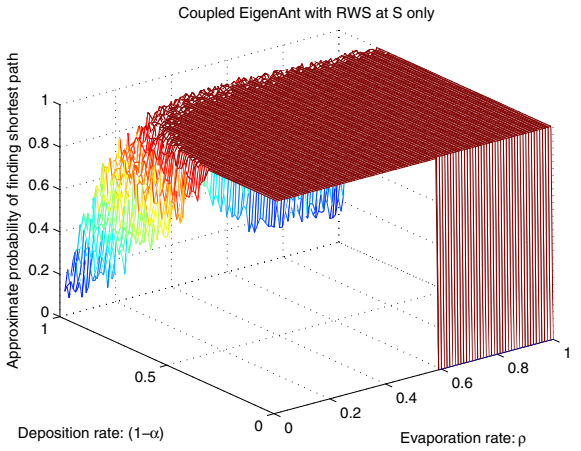

Fig. 10: Success probability as a function of removal and deposition rates for the Coupled EigenAnt algorithm, with flat initial conditions (= no initial bias), RWS at S only, and approximate probabilities based on 100 runs, for the 10 path problem (Elevation view). Simulation horizon of 1000 trips.

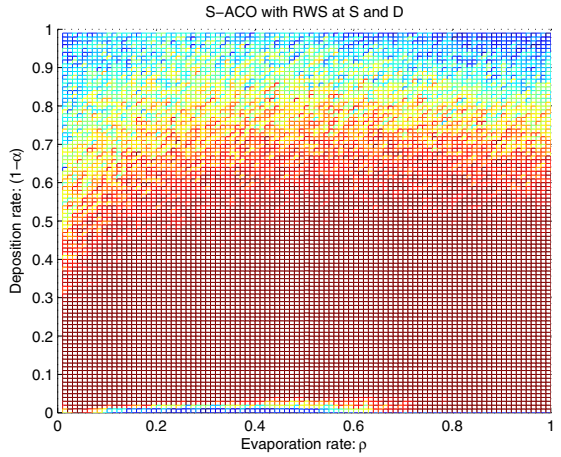

Fig. 9: Success probability as a function of removal and deposition rates for the S-ACO algorithm, with flat initial conditions (= no initial bias), RWS at S and D, and approximate probabilities based on 100 runs, for the 10 path problem (Plan view). Simulation horizon of 100 trips.

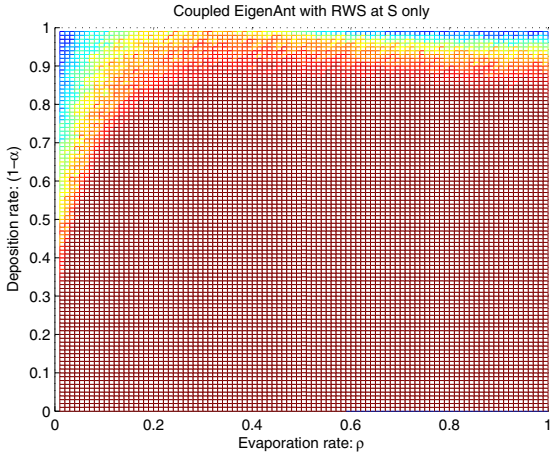

Fig. 11: Success probability as a function of removal and deposition rates for the Coupled EigenAnt, with flat initial conditions (= no initial bias), RWS at S only, and approximate probabilities based on 100 runs, for the 10 path problem (Plan view.). Simulation horizon of 1000 trips.

REFERENCES

[1] M. Dorigo and T. Stützle, *Ant Colony Optimization*. MIT Press, 2004.

[2] J.-L. Deneubourg, S. Aron, S. Goss, and J.-M. Pasteels, "The self-organizing exploratory pattern of the argentine ant." *Journal of Insect Behaviour*, vol. 3, pp. 159–168, 1990.

[3] Jayadeva, S. Shah, A. Bhaya, R. Kothari, and S. Chandra, "Ants find the shortest path: a mathematical proof," *Swarm Intelligence*, vol. 7, no. 1, pp. 43–62, 2013.

[4] C. Iacopino and P. Palmer, "The dynamics of ant colony optimization algorithms applied to binary chains," *Swarm Intelligence*, vol. 6, no. 4, pp. 343–377, 2012.

[5] P.-A. Bliman, A. Bhaya, E. Kaszkurewicz, and Jayadeva, "Convergence results for continuous-time dynamics arising in ant colony optimization," in *Proceedings of the 19th World Congress of the International Federation of Automatic Control*, Cape Town, 2014.

[6] A. Ezzat, A. M. Abdelbar, and D. C. Wunsch II, "A bare-bones ant colony optimization algorithm that performs competitively on the sequential ordering problem," *Memetic Computing*, pp. 1–11, 2014. [Online]. Available: http://dx.doi.org/10.1007/s12293-013-0129-z

[7] W. H. Bossert and E. Wilson, "The analysis of olfactory communication among animals," *Journal of Theoretical Biology*, vol. 5, pp. 443–469, 1963.

[8] C. Blum, "Ant colony optimization: Introduction and recent trends," *Physics of Life Reviews*, vol. 2, pp. 353–373, 2005.

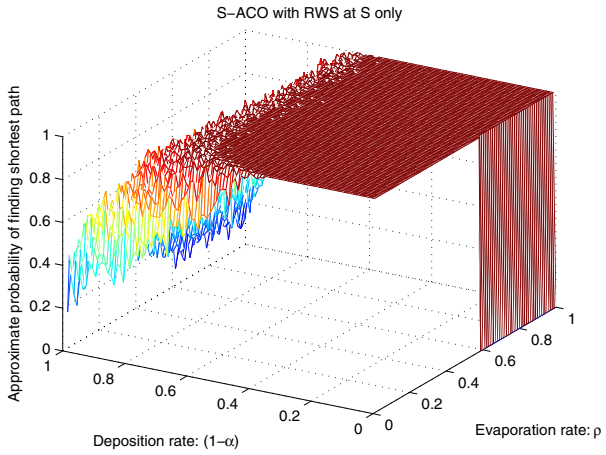

Fig. 12: Success probability as a function of removal and deposition rates for the S-ACO, with flat initial conditions (= no initial bias), RWS at S only, and approximate probabilities based on 100 runs (Elevation view). Simulation horizon of 1000 trips.

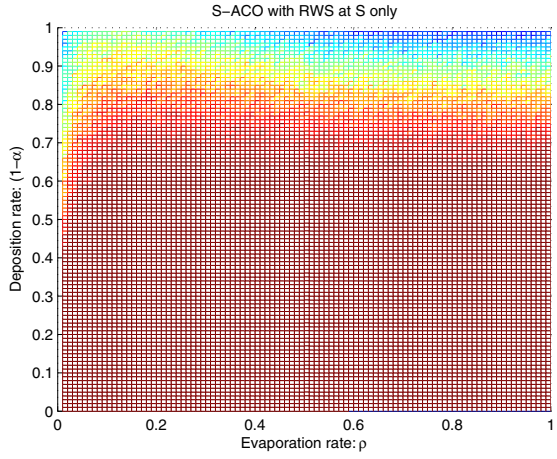

Fig. 13: Success probability as a function of removal and deposition rates for the S-ACO, with flat initial conditions (= no initial bias), RWS at S only, and approximate probabilities based on 100 runs. (Plan view). Simulation horizon of 1000 trips.